Peptide-Based Biomaterials for Protease-Enhanced Drug Delivery

Benedict Law, Ralph Weissleder, and Ching-Hsuan Tung*

Center of Molecular Imaging Research, Massachusetts General Hospital, Harvard Medical School, Charlestown, Massachusetts 02129

Received December 1, 2005; Revised Manuscript Received January 18, 2006

Controlled delivery of drugs in response to environments has the potential of targeting therapies and personalized treatments. Here, we described self-assembled peptide sequences that release therapeutic payloads upon specific interaction with disease-associated proteases. The core peptide sequence consists of a protease cleavable region flanked by two self-assembly motifs. In aqueous solution, the peptides self-assemble as a gel scaffold. With treatment of the model preparations with the appropriate protease, the matrix can be degraded in a controlled fashion, where the degradation rate is fine-tuned by varying the peptide compositions. Protease-mediated drug release was demonstrated by enzymatic treatment of a model therapeutic peptide incorporated into the optimized matrix. Our results suggest that this type of material may have far-reaching applications for functionally targeted drug delivery.

Introduction

The goal of any chemotherapy is to ensure the safety and efficient transportation of drug molecules to the targeted sites. During the past decade, advances in biotechnology enable us to design more sophisticated approaches for drug deliveries. For example, biological compounds such as peptides, proteins, and antibodies are employed to target angiogenesis.[1] Nanometer-sized particles are proposed for passive targeting of tumors.[2] Traditional materials used for drug deliveries are generally controlled and degraded by chemical reactions such as spontaneous hydrolysis of ester linkages. Biomaterials that are responsive to physiological stimulus and at the same time release an adaptable dosage may reduce treatment failure from pharmacogenomic differences of individual patients.[3]

Proteases are known to be involved in many physiological processes such as tissue remodeling,[4] wound healing,[5] and tumor invasion.[6−8] Thus, proteases have been identified as potential candidates to control drug release in vivo. A few meticulously engineered biomaterials that are sensitive to proteases have been prepared for various biomedical applications. Synthetic copolymers with the capacity to mimic matrix metalloproteinase-mediated invasion of the natural provisional matrix are useful in assisting tissue regeneration.[9,10] Quenched fluorescent polymers containing protease switches have been developed for medical imaging.[11] In addition, polymeric derivatives responding to proteolytic degradation were developed for drug delivery.[12] Anticancer drugs, for example, have been linked to polymer backbones through protease-specific peptide spacers, enabling selective drug release at tumor sites with high protease activity.[13−15] Here, we demonstrate a rational design of a new protease-responsive biomaterial. The protease-sensitive matrix is assembled by using building blocks, which contain a protease-sensitive motif and two weak β-sheet forming peptides sequences (Figure 1). The binary β-sheet peptides are able to form

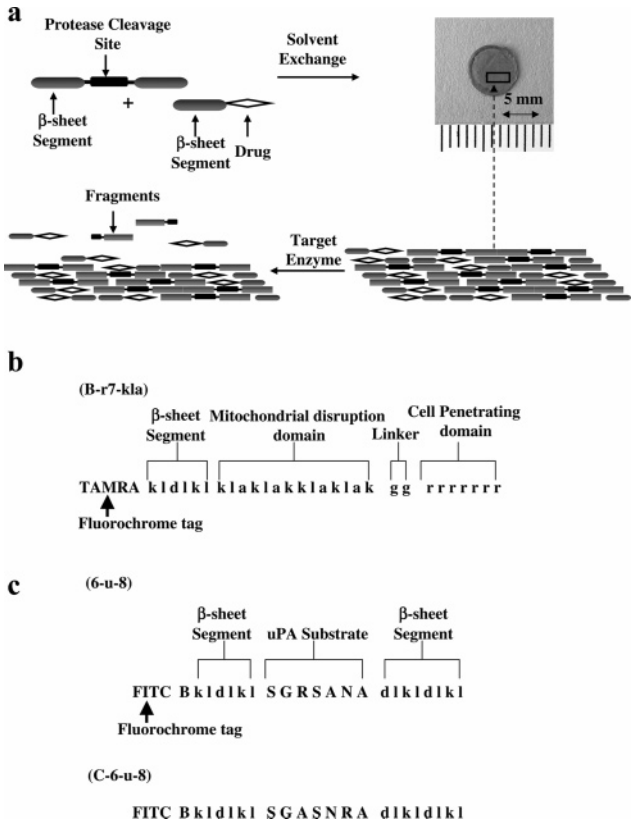

Figure 1. Design of the encapsulated enzyme releasable peptide-based matrix. (a) The core peptide sequence is composed of a protease cleavable region flanked by β-sheet forming motifs. In aqueous solution, peptides self-assemble into a gel matrix. Therapeutic agents can be encapsulated into this formulation. Upon addition of the targeted protease, the enzyme digests the preparations at the substrate cleavage site, resulting in release of gel fragments and therapeutic agents. (b) The optimized sequence of building block 6-u-8 and its nondegradable scramble control C-6-u-8. The designed peptide is cleaved selectively by uPA. (c) The composition of the therapeutic peptide, B-r7-kla, used in gel encapsulation. The fluorescent labels are added at the N-termini of the matrix and drug peptide sequences as the reporter molecules.

* To whom correspondence should be addressed: Center for Molecular Imaging Research, Massachusetts General Hospital, 149 13th Street, Room 5406, Charlestown, MA 02129. Tel: 617-726-5779. Fax: 617-726-5708. E-mail: tung@helix.mgh.harvard.edu.

10.1021/bm050920f CCC: $33.50
Published on Web 03/15/2006

self-assembled matrix via β-sheet stacking. Cleavage of the protease-sensitive sequence fragments the building blocks, on the gel surfaces to be cleaved, which in turn weakens the β-sheet interactions and results in matrix degradation.

Materials and Methods

Peptide Synthesis. Peptide synthesis was performed on an automated peptide synthesizer employing traditional N_α-Fmoc methodology. Fluorescein isothiocyanate (FITC) and 5-(and-6)-carboxytetramethylrhodamine (TAMRA) were attached to the N-termini of the peptide on resin as previously described.[16,17] Cleavage of peptides from the resin and side-chain deprotection employed a mixture of TFA/thioanisole/ethanedithiol/anisole 90/5/3/2 for 3 h at room temperature. Peptides were then precipitated by methyl-*tert*-butyl ether at 4 °C and purified by size exclusion chromatography in DMF. The collected fractions were further precipitated by diethyl ether and dried in vacuo. All peptides were characterized by MALDI-TOF mass spectrometry.

Protease-Assisted Matrix Degradation. Peptide analogues (1 mg/10 μL) dissolved in DMSO were added to a 96-well culture cluster plate in PBS buffer (200 μL). Yellow gels were formed immediately at the bottom of each well. After 24 h, the matrixes turned orange in color and were washed three times with PBS. To compare the degradations of different gel sequences, various analogues were incubated with uPA (100 nM) in PBS (200 μL) for 24 h. The sample solutions (100 μL) were transferred to a 96-well clear-bottom plate in PBS (100 μL). Fluorescence intensity measurements were recorded on a computer-controlled fluorescence plate reader. All data were acquired and analyzed by the installed computer software. For time course assays, preparations were made in a 96-well plate as described above. The samples were allowed to incubate with or without uPA (100 nM) in PBS (200 μL) for 24 h at room temperature. The sample solutions (100 μL) were transferred to a 96-well plate in PBS (100 μL) to measure the relative fluorescence intensities. The gels were then washed three times with PBS (200 μL). The procedures were repeated for four consecutive days. B-r7-kla encapsulated gel matrixes were prepared by using the same procedures, except B-r7-kla and 6-u-8 were mixed in DMSO prior to the matrixes formation.

MTS Assay. HT-1080 human fibrosarcoma cell lines supplied from American Type Culture Collection were cultured in 5% CO_2 at 37 °C. The HT-1080 fibrosacroma cells were incubated in DMEM supplemented with 10% (v/v) fetal bovine serum, glucose (4.5 g/L), L-glutamine (4 mM), nonessential amino acids (0.1 mM), sodium bicarbonate (1.5 g/L), penicillin (50,000 U/L), and streptomycin (0.05 g/L). Cells (5000/well) were seeded on a 96-well cell culture cluster plates for 12 h. Therapeutic peptides or solution mixtures from the gel degradations were added to individual wells and were incubated an additional 24 h. MTS solution (20 μL) was then added to individual wells. Samples were done in triplicate and the absorbance was measured at 490 nm. The results were recorded and analyzed by computer. The LD_{50} values were calculated by Prism software.

Results and Discussion

The KLD-12 peptide (Ac-KLDLKLDLKLDL) was previously reported to form stable β-sheet structures spontaneously in aqueous solution. Formation of these structures is induced by the repetitive alternating ionic hydrophilic and hydrophobic amino acids of the peptide.[18,19] Derivatives of this β-sheet forming peptide were used for preparation of membranes, nanotubes, and matrixes[20−22] To add sensitivity, a substrate peptide, SGRSANA, specific for urokinase plasminogen activator (uPA) was inserted between the KLD-12 self-assembly motifs. uPA was selected as a model protease because it plays an important role in extracellular matrix remodeling and facilitates cancer invasion into the surrounding tissues.[23−25]

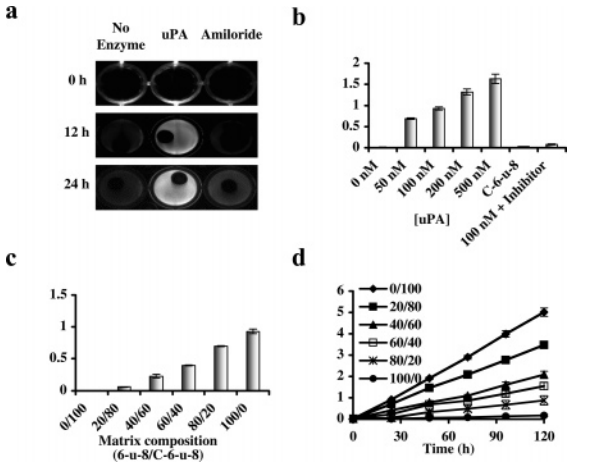

Figure 2. Response characteristics of the self-assembled matrixes. (a) Fluorescence image of 6-u-8. Matrixes were imaged in a 24-well plate as previously described. The images were taken 12 and 24 h after the addition of uPA (100 nM) in PBS buffer. Due to tight stacking of the building blocks, complete quenching of FITC was observed in the matrix. The fluorescence signal was restored after release from the matrix by uPA activity. (b) Percentage increase in fluorescence signal versus various uPA concentration (0−500 nM). The increase in fluorescence emission is enzyme-dependent. Amiloride (1 mM) was used as the inhibitor. The same amount of uPA (100 nM) was added to both the C-6-u-8 and inhibition experiments. Fold increased in fluorescence = $[F_1/F_0 - 1]$. (c) Comparison of the degradation ratios for matrixes containing different compositions of 6-u-8 and C-6-u-8 24 h after addition of uPA (100 nM). (d) Degradation of the matrixes containing different compositions of 6-u-8 and C-6-u-8 with time (per 24 h).

Clinically, elevated uPA in malignant breast, gastrointestinal, and urogenital tumors indicate poor diseases prognosis.[26] In primary breast cancer, high tumor levels of uPA are associated with poor overall survival.[27,28] The synthetic substrate (SGRSANA) is known to be 840 times more efficient in uPA cleavage (k_{cat}/K_m = 1200 M^{-1} s^{-1}) than the native sequence from plasminogen[29] and was used previously to prepare a uPA-sensitive fluorescence probe.[16]

The self-assembled peptide matrixes are prepared by solvent exchange and can be molded in a casting frame. A fluorescein isothiocyanate (FITC) tag was covalently attached to the N-terminus of the building blocks as a reporter to monitor degradation of the matrix. An initial screen was performed to activate the protease-mediated release of the building blocks with various lengths of β-sheet forming segments, extending from 6 to 10 residues at both C- and N-termini of the assembly motifs (Supporting Information). From this study, it is evident that variation of the self-assembly motif length is not a predictable approach for controlling the degradation rates. As the length of the β-sheet forming segment is increased, the digested peptides may remain attached onto the scaffolds by hydrophobic interactions. The optimized building block 6-u-8, KLDLKL-SGRSANA-DLKLDLKL, was found to be the most sensitive matrix to the target uPA protease (Figure 1b). This sequence was found to consist 40% of β-sheet structure (Supporting Information). The resulting preparations have a strong orange color, indicating high fluorochrome content, but they are fluorescently silent (excitation at 460−480 nm and emission at 520−540 nm) (Figure 2a). Complete quenching of the fluorescein emission is attributed to the tight β-sheet structure. After incubation of the matrix with uPA (100 nM) for 12 and 24 h, increased fluorescence emission, indicating the release of FITC-containing peptide fragments into the buffer, was observed. The wells containing amiloride (1 mM), an uPA

Table 1. Degradation and Release of Drug-Containing Matrix[a]

components matrix/drug (% v/v)	absorbance at 495 nm matrix		degradation (fold)	absorbance at 555 nm drug		drug release (fold)
	no enzyme	enzyme		no enzyme	enzyme	
100/0	0.78 ± 0.11	1.91 ± 0.23	2.45	0.00 ± 0.00	0.00 ± 0.00	
80/20	0.54 ± 0.04	1.14 ± 0.11	2.11	0.10 ± 0.01	0.18 ± 0.01	1.80
60/40	0.51 ± 0.06	0.92 ± 0.11	1.80	0.13 ± 0.02	0.19 ± 0.01	1.46
40/60	0.39 ± 0.07	0.66 ± 0.14	1.69	0.10 ± 0.01	0.14 ± 0.02	1.40
20/80	0.22 ± 0.06	0.34 ± 0.11	1.54	0.07 ± 0.03	0.06 ± 0.01	0.85

[a] Various preparations ($n = 3$) contain different components of 6-u-8 and B-r7-kla. Identical amounts of peptide (1 mg/μL) were used for the gel formations in a 96-well plate. After incubation with uPA (100 nM) in PBS for 24 h at 25 °C, buffer solutions (100 μL) were diluted with PBS (300 μL). The release of the digested matrix fragments and B-r7-kla from all preparations was quantified by absorbance at 495 and 555 nm, respectively. The fold increased in absorbance of a particular preparation was calculated by dividing the background signal of the correspondent analogue without uPA.

inhibitor,[30] show only a trace amount of fluorescence emission, suggesting the observed fluorescence is specific to uPA activity. Gel degradation is uPA concentration-dependent; fluorescence emission increased with increasing uPA concentrations (Figure 2b). As previously observed, only a slight increase in fluorescence emission was found when amiloride inhibitor was added (1 mM). To further confirm the selectivity of 6-u-8 to uPA, the building block C-6-u-8 was synthesized by replacing the substrate cleavage site with a scrambled sequence (SGASNRA) (Figure 1b).[16,31] As expected, the C-6-u-8 matrix containing the scrambled sequence did not show degradation upon addition of uPA (100 nM) (Figure 2b).

Given the difference in stability between 6-u-8 and C-6-u-8 sequences allows for rational design of controlled-release hydrogels. Matrix analogues were prepared by formulating different ratios of 6-u-8 and C-6-u-8. As expected, the degradation rates correlate with the proportion of 6-u-8 in the gel matrix. Preparations with a higher percentage of 6-u-8 were more likely to be digested by uPA (Figure 2c). Time course experiments show that the degradation rates decrease with increasing C-6-u-8 proportions (Figure 2d). Our results support the hypothesis that by mixing the degradable 6-u-8 with the nondegradable C-6-u-8, the degradation rates can be controlled, thus affording the ability to fine-tune the desired degradation kinetics.

To demonstrate potential drug delivery applications of the biomaterial, a mitochondrial disruption peptide, klaklakklaklak (kla), was encapsulated into the gel matrix. Previously, this peptide was shown to induce apoptosis in tumor cells.[32−34] A membrane penetrating polyarginine peptide, rrrrrrr, was tethered to the C-terminus of kla peptide for enhanced intracellular delivery, and a β-sheet forming segment (kldlkl) was added to the N-terminus to facilitate a β-sheet stacking (Figure 1c). The whole peptide (B-r7-kla) was synthesized using D-amino acids to prevent metabolic degradation in vivo. In addition, carboxytetramethylrhodamine (TAMRA) was added as a reporter to monitor drug release by absorbance spectroscopy. Prior to any investigations, the cytotoxicity of B-r7-kla to HT-1080 human fibrosarcoma cell lines was confirmed with the MTS assay.[35] The obtained IC_{50} value was 6.2 μM (Supporting Information).

To study the drug release efficiency, matrixes were formulated with various ratios of 6-u-8 and B-r7-kla (% v/v). The casted matrixes were then incubated with equal amount of uPA. To avoid potential Förster fluorescence resonance energy transfer (FRET) from the FITC to TAMRA, peptides were quantified simultaneously by UV absorbance at 495 and 555 nm, which correspond to the presence of FITC from the gel matrixes and TAMRA from the B-r7-kla drug, respectively. Matrix degradation increased inversely with the ratio of 6-u-8 (Table 1). This may be the result of decreasing the number of the available uPA-cleavage sites on the gel surface available for enzyme cleavage. Enhanced drug release is observed to correlate with increased degradation of the gel matrix.

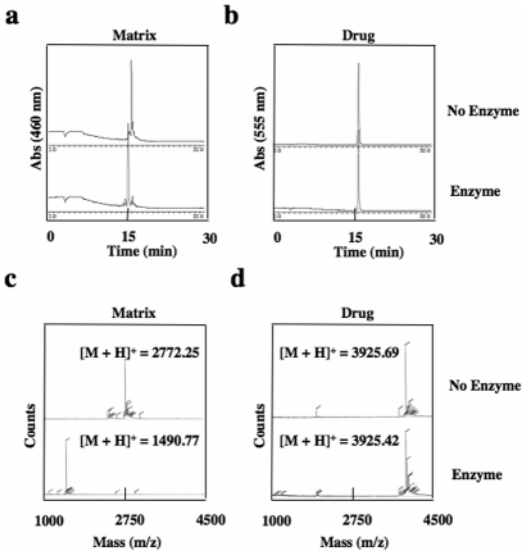

Figure 3. Characterization of the encapsulated matrix formulations. After enzyme treatment (100 nM), the solution mixtures were injected and analyzed by RP-HPLC. For ease of comparison, peptide amounts were normalized in accordance with the concentrations of fluorophores prior to HPLC injection. Absorbance at (a) 460 nm and (b) 555 nm indicates release of matrix fragments and B-r7-kla, respectively. The 6-u-8 fragment was identified as a fast-eluting peak. Analysis of the HPLC fractions by MALDI-TOF spectrometry (c and d).

The mechanism of protease-assisted drug release was further confirmed by reverse-phase HPLC and mass spectrometry. Elution peaks were monitored by the absorbance of FITC and TAMRA, representing the matrix and the drug, respectively. In the presence of uPA, an early-eluted new peak with FITC absorbance was found, suggesting 6-u-8 was cleaved by uPA (Figure 3a). MALDI-TOF MS analysis gave a single peak at 1490.77 Da, representing $[M + H]^+$ mass ion of FITC-Bkldlkl-SGR the cleaved fragments (Figure 3c). As previously described, the enzyme cleavage site was located between the arginine and serine residues.[29] Meanwhile, the B-r7-kla peptide remained intact. No degradation of the drug peptide was observed in the activated and nonactivated matrixes. This was shown by the overlapping HPLC spectra (Figure 3b) and confirmed by the mass spectrometry (Figure 3d).

Next, enzyme activation kinetics of preparation 6-u-8/B-r7-kla:80/20 were investigated. Different concentrations of uPA (0−500 nM) were added (at $t = 8$ h) to investigate the matrix degradation (Figure 4a and b). Samples were incubated for 8 h with uPA. Degradation of the gels is uPA-dependent, but the maximum dissociation of 6-u-8 fragments from the matrixes

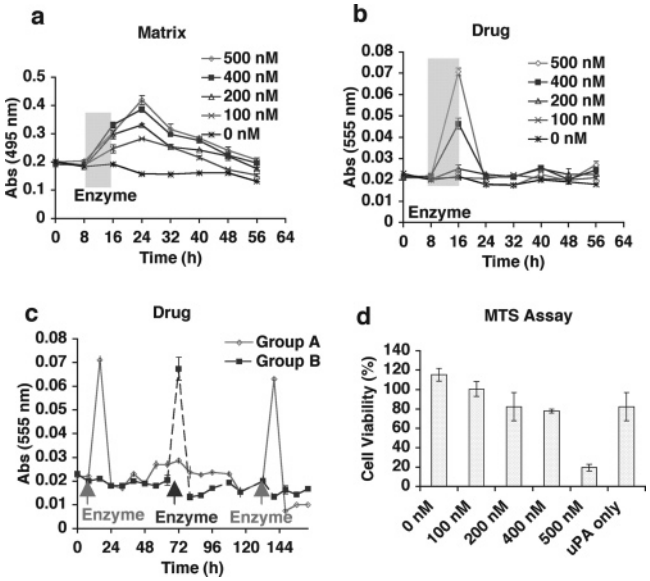

Figure 4. Drug release of the encapsulated matrix formulations. Matrixes were incubated with PBS (200 μL) at room temperature. Buffers were changed every 8 h. The solution mixtures (100 μL) were collected and diluted with PBS (300 μL) to monitor the absorbance at (a) 495 nm and (b) 555 nm, which corresponded to the release of the matrix fragments and the therapeutic B-r7-kla peptide, respectively. Various final concentrations of uPA (0−500 nM) were added at $t = 8$ h. (c) Two groups (A and B, $n = 6$) of gels were prepared to be activated by uPA (500 nM) at specific time points. The gels demonstrated pulse-release properties. (d) Solution mixtures from gel samples (100 μL) at $t = 16$ from (b) were added to HT-1080 cell lines (5000/well) in a culture medium (100 μL) and incubated for 24 h in 5% CO_2 at 37 °C. Cell viability was determined by adding 20 μL of MTS solution. Absorbance at 490 nm was measured, and the LD_{50} values were calculated from the growth curves. Results are the average of three independent experiments, $P < 0.05$, t-test.

was delayed for 8 h in all samples with enzymes, as indicated by the peak absorptions at $t = 24$ h. On the other hand, the encapsulated B-r7-kla was released almost instantly with uPA (Figure 4b). Maximum absorbance was found at $t = 16$ h (Figure 4b) and immediately returned to the background levels after enzyme removal. The delayed gel degradation kinetics could be attributed to the hydrophobic interaction of the peptide fragments to the matrixes. Despite the different kinetic profiles of matrix degradations, the system demonstrates the enzyme-assisted drug release effects were digitized. To demonstrate this principal, gels ($n = 6$) were separated into two groups and were activated at specific time points. The release of B-r7-kla from the matrix could be controlled at any given time point by addition of enzyme and was only observed in the presence of the enzymes (Figure 4c). The cytotoxcity of the solution obtained from uPA-dependent release using HT-1080 cell lines was investigated. With no enzyme, the encapsulated B-r7-kla was released slowly and no cytotoxic effects were observed (Figure 4d). High uPA concentrations (500 nM), however, significantly enhanced drug release. After 24 h, the fraction of variable cells was reduced to 18%.

Conclusions

In summary, peptide-based matrixes with varying uPA sensitivities have been synthesized and tested. The materials were constructed from biologically inspired peptide sequences and were labeled with fluorescein for physiochemical studies. Unlike traditional synthetic materials, which are usually degraded by chemical reactions, such as ester hydrolysis,[36,37] degradation of our matrixes proceed via dose-dependent enzymatic cleavage and dissolution. The degradation pattern can be adjusted by varying the ratios of different components of the gels and thus control the rate of matrix degradation. Initial toxicity assay indicated the prepared matrixes are nontoxic in vitro. Such an approach may be applied for making controlled or enhanced release preparations, especially for preparing hybrid materials for drug delivery.[38] In addition, the approach may be adapted to prepare similar biomaterials for additional proteases. Overall, our data suggested that this type of material could have far-reaching applications for targeted and functional drug delivery. We believe biomaterials that are responsive to physiological stimulus and have the ability to release an adaptable dosage may lead to successful treatments.

Acknowledgment. The authors would like to thank Dr. Scott Hilderbrand for editorial assistance. This research was supported by NIH P50-CA86355, RO1 CA99385, and DOD DC044945.

Supporting Information Available. Screening of building blocks, LD50 of B-r7-kla and CD spectrum. This material is available free of charge via the Internet at http://pubs.acs.org.

References and Notes

(1) Alessi, P.; Ebbinghaus, C.; Neri, D. *Biochim. Biophys. Acta* **2004**, *1654*, 39−49.
(2) Moghimi, S. M.; Hunter, A. C.; Murray, J. C. *Faseb. J.* **2005**, *19*, 311−30.
(3) Sadee, W.; Dai, Z. *Hum. Mol. Genet*. **2005**, *14* Suppl. 2, R207-14.
(4) Liu, J.; Sukhova, G. K.; Sun, J. S.; Xu, W. H.; Libby, P.; Shi, G. P. *Arterioscler. Thromb. Vasc. Biol.* **2004**, *24*, 1359−66.
(5) Macfarlane, S. R.; Seatter, M. J.; Kanke, T.; Hunter, G. D.; Plevin, R. *Pharmacol. Rev.* **2001**, *53*, 245−82.
(6) DeClerck, Y. A.; Mercurio, A. M.; Stack, M. S.; Chapman, H. A.; Zutter, M. M.; Muschel, R. J.; Raz, A.; Matrisian, L. M.; Sloane, B. F.; Noel, A.; Hendrix, M. J.; Coussens, L.; Padarathsingh, M. *Am. J. Pathol.* **2004**, 164, 1131−9.
(7) Lee, M.; Fridman, R.; Mobashery, S. *Chem. Soc. Rev.* **2004**, *33*, 401−9.
(8) Joyce, J. A.; Baruch, A.; Chehade, K.; Meyer-Morse, N.; Giraudo, E.; Tsai, F. Y.; Greenbaum, D. C.; Hager, J. H.; Bogyo, M.; Hanahan, D. *Cancer Cell* **2004**, *5*, 443−53.
(9) Hubbell, J. A. *Curr. Opin. Biotechnol.* **1999**, *10*, 123−9.
(10) Lutolf, M. P.; Lauer-Fields, J. L.; Schmoekel, H. G.; Metters, A. T.; Weber, F. E.; Fields, G. B.; Hubbell, J. A. *Proc. Natl. Acad. Sci. U.S.A.* **2003**, *100*, 5413−8.
(11) Tung, C. H. *Biopolymers* **2004**, *76*, 391−403.
(12) Duncan, R. *Nat. Rev. Drug Discov.* **2003**, *2*, 347−60.
(13) Putnam, D.; Kopecek, J. *Bioconjug. Chem.* **1995**, *6*, 483−92.
(14) Chau, Y.; Tan, F. E.; Langer, R. *Bioconjug. Chem.* **2004**, *15*, 931−41.
(15) Satchi-Fainaro, R.; Puder, M.; Davies, J. W.; Tran, H. T.; Sampson, D. A.; Greene, A. K.; Corfas, G.; Folkman, J. *Nat. Med.* **2004**, *10*, 255−61.
(16) Law, B.; Curino, A.; Bugge, T. H.; Weissleder, R.; Tung, C. H. *Chem. Biol.* **2004**, *11*, 99−106.
(17) Law, B.; Weissleder, R.; Tung, C. H. *Chembiochem* **2005**, *6*, 1361−7.
(18) Kisiday, J.; Jin, M.; Kurz, B.; Hung, H.; Semino, C.; Zhang, S.; Grodzinsky, A. J. *Proc. Natl. Acad. Sci. U.S.A.* **2002**, *99*, 9996−10001.
(19) Xiong, H.; Buckwalter, B. L.; Shieh, H. M.; Hecht, M. H. *Proc. Natl. Acad. Sci. U.S.A.* **1995**, *92*, 6349−53.
(20) Zhang, S.; Holmes, T.; Lockshin, C.; Rich, A. *Proc. Natl. Acad. Sci. U.S.A.* **1993**, *90*, 3334−8.
(21) Zhang, S.; Holmes, T. C.; DiPersio, C. M.; Hynes, R. O.; Su, X.; Rich, A. *Biomaterials* **1995**, *16*, 1385−93.
(22) Holmes, T. C.; de Lacalle, S.; Su, X.; Liu, G.; Rich, A.; Zhang, S. *Proc. Natl. Acad. Sci. U.S.A.* **2000**, *97*, 6728−33.
(23) Edwards, D. R.; Murphy, G. *Nature* **1998**, *394*, 527−8.

(24) Johnsen, M.; Lund, L. R.; Romer, J.; Almholt, K.; Dano, K. *Curr. Opin. Cell Biol.* **1998**, *10*, 667−71.
(25) Koblinski, J. E.; Ahram, M.; Sloane, B. F. *Clin. Chim. Acta* **2000**, *291*, 113−35.
(26) Harbeck, N.; Alt, U.; Berger, U.; Kruger, A.; Thomssen, C.; Janicke, F.; Hofler, H.; Kates, R. E.; Schmitt, M. *Clin. Cancer Res.* **2001**, *7*, 2757−64.
(27) Janicke, F.; Prechtl, A.; Thomssen, C.; Harbeck, N.; Meisner, C.; Untch, M.; Sweep, C. G.; Selbmann, H. K.; Graeff, H.; Schmitt, M. *J. Natl. Cancer Inst.* **2001**, *93*, 913−20.
(28) Look, M. P.; van Putten, W. L.; Duffy, M. J.; Harbeck, N.; Christensen, I. J.; Thomssen, C.; Kates, R.; Spyratos, F.; Ferno, M.; Eppenberger-Castori, S.; Sweep, C. G.; Ulm, K.; Peyrat, J. P.; Martin, P. M.; Magdelenat, H.; Brunner, N.; Duggan, C.; Lisboa, B. W.; Bendahl, P. O.; Quillien, V.; Daver, A.; Ricolleau, G.; Meijer-van Gelder, M. E.; Manders, P.; Fiets, W. E.; Blankenstein, M. A.; Broet, P.; Romain, S.; Daxenbichler, G.; Windbichler, G.; Cufer, T.; Borstnar, S.; Kueng, W.; Beex, L. V.; Klijn, J. G.; O'Higgins, N.; Eppenberger, U.; Janicke, F.; Schmitt, M.; Foekens, J. A. *J. Natl. Cancer Inst.* **2002**, *94*, 116−28.
(29) Ke, S. H.; Coombs, G. S.; Tachias, K.; Corey, D. R.; Madison, E. L. *J. Biol. Chem.* **1997**, *272*, 20456−62.
(30) Klinghofer, V.; Stewart, K.; McGonigal, T.; Smith, R.; Sarthy, A.; Nienaber, V.; Butler, C.; Dorwin, S.; Richardson, P.; Weitzberg, M.; Wendt, M.; Rockway, T.; Zhao, X.; Hulkower, K. I.; Giranda, V. L. *Biochemistry* **2001**, *40*, 9125−31.
(31) Law, B.; Hsiao, J. K.; Bugge, T. H.; Weissleder, R.; Tung, C. H. *Anal. Biochem.* **2005**, *338*, 151−8.
(32) Javadpour, M. M.; Juban, M. M.; Lo, W. C.; Bishop, S. M.; Alberty, J. B.; Cowell, S. M.; Becker, C. L.; McLaughlin, M. L. *J. Med. Chem.* **1996**, *39*, 3107−13.
(33) Ellerby, H. M.; Arap, W.; Ellerby, L. M.; Kain, R.; Andrusiak, R.; Rio, G. D.; Krajewski, S.; Lombardo, C. R.; Rao, R.; Ruoslahti, E.; Bredesen, D. E.; Pasqualini, R. *Nat. Med.* **1999**, *5*, 1032−8.
(34) Mai, J. C.; Mi, Z.; Kim, S. H.; Ng, B.; Robbins, P. D. *Cancer Res.* **2001**, *61*, 7709−12.
(35) Cory, A. H.; Owen, T. C.; Barltrop, J. A.; Cory, J. G. *Cancer Commun.* **1991**, *3*, 207−12.
(36) Suggs, L. J.; Mikos, A. G. *Cell Transplant* **1999**, *8*, 345−50.
(37) Saito, N.; Okada, T.; Horiuchi, H.; Murakami, N.; Takahashi, J.; Nawata, M.; Ota, H.; Nozaki, K.; Takaoka, K. *Nat. Biotechnol.* **2001**, *19*, 332−5.
(38) Vandermeulen, G. W.; Klok, H. A. *Macromol. Biosci.* **2004**, *4*, 383−98.

BM050920F